

# Exploring CLIP’s Dense Knowledge for Weakly Supervised Semantic Segmentation

Zhiwei Yang<sup>1,2</sup> Yucong Meng<sup>2,3</sup>

Kexue Fu<sup>4</sup> Feilong Tang<sup>1</sup> Shuo Wang<sup>2,3\*</sup> Zhijian Song<sup>1,2,3\*</sup>

<sup>1</sup>Academy for Engineering and Technology, Fudan University, Shanghai 200433, China

<sup>2</sup>Shanghai Key Laboratory of Medical Image Computing and Computer Assisted Intervention

<sup>3</sup>Digital Medical Research Center, School of Basic Medical Sciences, Fudan University, China

<sup>4</sup>Shandong Computer Science Center (National Supercomputer Center in Jinan)

## Abstract

Weakly Supervised Semantic Segmentation (WSSS) with image-level labels aims to achieve pixel-level predictions using Class Activation Maps (CAMs). Recently, Contrastive Language-Image Pre-training (CLIP) has been introduced in WSSS. However, recent methods primarily focus on image-text alignment for CAM generation, while CLIP’s potential in patch-text alignment remains unexplored. In this work, we propose ExCEL to explore CLIP’s dense knowledge via a novel patch-text alignment paradigm for WSSS. Specifically, we propose Text Semantic Enrichment (TSE) and Visual Calibration (VC) modules to improve the dense alignment across both text and vision modalities. To make text embeddings semantically informative, our TSE module applies Large Language Models (LLMs) to build a dataset-wide knowledge base and enriches the text representations with an implicit attribute-hunting process. To mine fine-grained knowledge from visual features, our VC module first proposes Static Visual Calibration (SVC) to propagate fine-grained knowledge in a non-parametric manner. Then Learnable Visual Calibration (LVC) is further proposed to dynamically shift the frozen features towards distributions with diverse semantics. With these enhancements, ExCEL not only retains CLIP’s training-free advantages but also significantly outperforms other state-of-the-art methods with much less training cost on PASCAL VOC and MS COCO. Code is available at <https://github.com/zwyang6/ExCEL>.

## 1. Introduction

Weakly Supervised Semantic Segmentation (WSSS) intends to generate pixel-level predictions using weak annotations like points [2], scribbles [18, 32], bounding boxes [8,

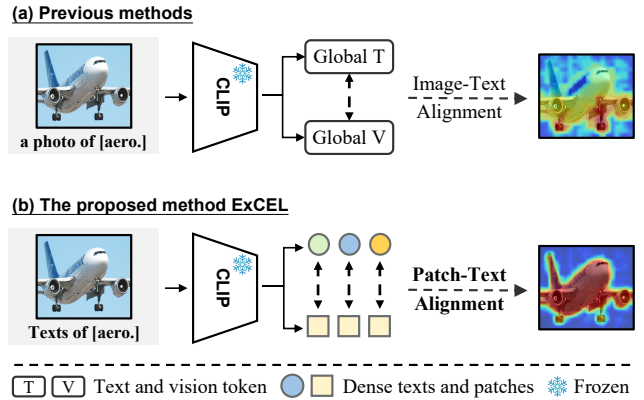


Figure 1. Our motivation. (a) Previous methods leverage CLIP to generate CAMs with global image-text alignment, leaving CLIP’s dense knowledge unexplored. (b) The proposed ExCEL explores CLIP’s dense knowledge via a novel patch-text alignment paradigm, which generates better CAMs with less training cost.

16], or image-level labels [1, 23, 40]. It significantly reduces the annotating cost of fully supervised methods and has attracted increasing attention in the community. Among all cheap annotation types, most WSSS approaches leverage image-level labels to provide dense localization cues, linking visual concepts to specific pixel regions [5, 33]. In this work, we focus on WSSS with image-level labels as well.

Commonly, the WSSS pipeline involves three stages: generating Class Activation Maps (CAMs) [46] by training a classification network, refining CAMs into pseudo labels [28], and using these labels to train a segmentation model [7]. However, due to the minimal semantic information from image-level labels, CAMs intend to highlight the most distinctive object parts, significantly limiting WSSS performance. Recently, Contrastive Language-Image Pre-training (CLIP) [24] has been introduced in WSSS. CLIMs [36] applies image-text pairs to regularize visual relations among different semantics. CLIP-ES [20]

\*Corresponding authors. Email: {shuowang, zjsong}@fudan.edu.cn.

leverages image-text alignment for gradient and produces high-quality GradCAM [30]. WeCLIP [43] further streamlines this process by using CLIP’s visual encoder for segmentation. Despite these advancements, current methods primarily focus on CLIP’s global image-text alignment, as shown in Fig. 1 (a). CLIP’s dense knowledge with patch-text alignment still remains under-explored in WSSS.

In this work, we propose ExCEL to explore CLIP’s dense knowledge via a patch-text alignment paradigm for WSSS, i.e., generating CAMs by calculating patch-wise similarity between text and individual patch tokens, as shown in Fig. 1 (b). We identify two key challenges: (1) Semantic sparsity in textual prompts, where the template ‘a photo of [CLASS]’ only indicates object presence but lacks knowledge for localization, and (2) Fine-grained insufficiency in visual features, as CLIP prioritizes global representation due to its image-text pairing nature. To address these, ExCEL enhances CLIP’s dense alignment with Text Semantic Enrichment (TSE) and Visual Calibration (VC) modules, unlocking its potential across text and vision modalities.

To generate semantically rich text representations, we propose TSE through an implicit attribute feature space. Instead of relying on explicit text templates, TSE module implicitly constructs text embeddings using universal attributes across the dataset. We first employ Large Language Models (LLMs) to generate detailed descriptions for each class, which are then processed by CLIP’s text encoder to build a dataset-wide knowledge base. Rather than directly fusing these class-specific descriptions for text prompting, we focus on clustering the descriptive embeddings into generalized attributes, which effectively capture complementary knowledge from other classes and supplement missing information for the target class. With this implicit feature space, we enhance the text embeddings by hunting for its most relevant attribute features and aggregate them into the final class-specific text representation. This approach enables TSE to generate more informative text embeddings, providing a strong foundation for visual recognition.

To mine fine-grained knowledge from visual features, we propose VC to calibrate CLIP in both non-trainable and efficient-learnable ways. Our findings suggest that CLIP’s q-k attention loses fine-grained details. Therefore, we first propose a Static Visual Calibration (SVC) module to replace the suboptimal q-k attention with a straightforward Intra-correlation operation. It focuses on extracting fine-grained details from intermediate layers, which progressively propagates fine-grained visual knowledge. Without any retraining, SVC generates CAMs comparable to training-required WSSS methods. Building on this, we further propose a Learnable Visual Calibration (LVC) module to dynamically calibrate CLIP’s frozen features. LVC extracts spatial correlations from SVC’s static CAMs. These correlations further supervise a lightweight adapter to learn

the dynamic shift, pushing frozen features towards spatial-aware distributions. LVC and SVC complement each other, enabling precise patch-text alignment for CAM generation.

The main contributions of our work are listed as follows:

- We explore CLIP’s dense knowledge via a novel patch-text alignment paradigm for WSSS. The proposed ExCEL generates better pseudo labels in both training-free and efficient learning manners, revealing the dense capabilities of CLIP for efficient CAM generation.
- To enhance patch-text alignment, we propose the Text Semantic Enrichment (TSE) and Visual Calibration (VC) modules. TSE applies LLMs to build a dataset-wide knowledge base and treats text prompting as an implicit attribute-hunting process, making text embeddings more informative. VC propagates the fine-grained visual knowledge in a non-parametric manner and further dynamically calibrates the frozen features with a lightweight adapter. TSE and VC work across two modalities, generating better dense alignment and pseudo labels.
- Extensive experiments on PASCAL VOC and MS COCO demonstrate that ExCEL significantly outperforms recent state-of-the-art methods, while reducing training cost with only 3.2 GB of GPU memory and 6% of the training time required by recent methods.

## 2. Related Works

### 2.1. Weakly Supervised Semantic Segmentation

Weakly supervised semantic segmentation with image-level labels typically relies on CAMs to provide dense supervision for segmentation [42, 44]. However, CAMs usually highlight the most discriminative parts of objects [34]. To address this issue, considerable efforts have been made from many intriguing insights. MCTformer [37] incorporates multiple class tokens in Vision Transformer and proposes generating CAMs from class-patch attention. ToCo [29] proposes token contrast learning and generates more precise CAMs. SeCo [39] designs a separate and conquer scheme and succeeds in tackling co-occurrence. Despite these advancements, prior methods commonly require retraining the entire classification network for CAM generation. In this work, our ExCEL directly generates CAMs from frozen CLIP, and further boosts its quality via a lightweight adapter, significantly reducing the training cost.

### 2.2. Vision-Language Pre-training

Contrastive Language Image Pre-training (CLIP) [24], known for pretraining on billion-scale image-text pairs, has demonstrated remarkable transferability in many downstream tasks. CoOP [48] and CLIP-Adapter [12] incorporate lightweight trainable parameters into CLIP and succeed in few-shot classification. DenseCLIP [25] and

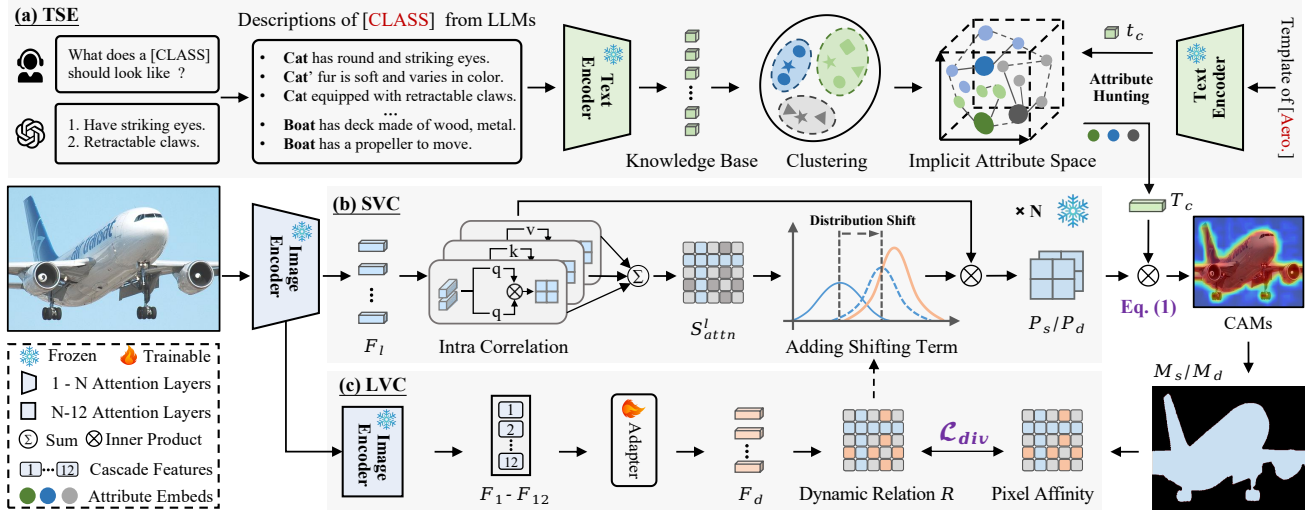


Figure 2. ExCEL Architecture. We explore CLIP’s dense knowledge with Text Semantic Enrichment (TSE) and Visual Calibration (VC). (a) TSE uses LLMs to build a knowledge base and clusters it into an implicit attribute space. The final text representation  $T_c$  is enhanced by hunting for relevant attributes. For vision modality, (b) we introduce Static Visual Calibration (SVC) to calibrate visual features using the Inter-correlation operation across  $N$  intermediate layers. It generates static CAMs with  $T_c$  and calibrated features  $P_s$ . (c) Learnable Visual Calibration (LVC) designs a learnable adapter to add a dynamic shift  $R$  to SVC. It generates optimized features  $P_d$  based on static CAMs guidance, creating dynamic CAMs from  $P_d$  and  $T_c$ . Dynamic CAMs are refined for segmentation supervision. Details are in Sec. 3.1.

MaskCLIP [47] leverage the alignment between text and vision modalities for the dense segmentation task. Recently, some studies have introduced CLIP into WSSS. CLIMS [36] treats image-text pairing of CLIP as regularization and leverages it to regularize the visual concepts. CLIP-ES [20] finds that the image-text alignment of CLIP generates class gradient and leverages it for GradCAM generation. WeCLIP [43] further streamlines this process and directly leverages CLIP’s visual encoder for segmentation. However, these methods mainly focus on a global image-text alignment while ignoring the dense capabilities of CLIP. In contrast, our ExCEL explores CLIP’s dense knowledge via a patch-text alignment paradigm for WSSS.

### 3. Methodology

#### 3.1. Preliminaries

**Patch-text CAM Generation.** CLIP uses image and text encoders to project image and text into the same feature space, enabling robust vision-language alignment. In this work, we utilize this property to generate CAM in a patch-text alignment paradigm. Given the encoded text embeddings  $T \in \mathbb{R}^{D \times C}$  and visual features  $P \in \mathbb{R}^{h \times w \times D}$ , where  $D$  is the feature channel,  $h$  and  $w$  are the spatial sizes,  $C$  is the number of classes, we generate CAM by calculating the patch-wise similarities between text and visual features:

$$\text{CAM} = \text{Norm}(\cos(P, T)), \quad (1)$$

where  $\text{Norm}(\cdot)$  is the min-max normalization and  $\cos(\cdot)$  is the cosine similarity calculation. However, due to

the image-level pairing nature, CLIP suffers from textual semantic sparsity and visual fine-grained insufficiency. Therefore, our ExCEL incorporates TSE and VC (SVC and LVC) into CLIP to further explore its dense potential.

**Framework Overview.** Our ExCEL generates CAMs in both training-free and efficient learning manners, as shown in Fig. 2. Its training pipeline is generalized as follows:

- (1) Enriching textual semantics via TSE. We first use GPT-4 to generate descriptions for each class, which are encoded into a dataset-wide knowledge base with CLIP’s text encoder. We cluster this knowledge into class-agnostic attributes and use the global text prompt to hunt for its most relevant ones. They are then aggregated into the final text representation.
- (2) Static CAM generation via SVC. We replace CLIP’s q-k self-attention with our Intra-correlation operation from intermediate layers. Then the calibrated visual features and enhanced text embeddings are used for static CAMs via Eq. (1).
- (3) Dynamic CAM generation via LVC. A lightweight adapter is designed to learn dynamic token relations from static CAMs. The relations are added to SVC and serve as a distribution shift to make the visual features more diverse. The dynamic CAMs are generated with the enhanced text embeddings and LVC features via Eq. (1).
- (4) Segmentation training. Dynamic CAMs are refined to pseudo labels for segmentation supervision.

#### 3.2. Text Semantic Enrichment

**Knowledge Base Construction.** The global text template ‘a clean origami of [CLASS]’ only indicates the presence of objects while limited providing dense knowledge for

patch-wise visual recognition. To enrich the text representation, we first adapt LLMs, such as GPT-4 to generate detailed class descriptions, as shown in Fig. 2 (a). Specifically, given the global template  $E_c$  from class label space  $Y \in \{1, 2, \dots, C\}$ , where  $c$  is the class index and  $C$  is the number of categories, we carefully construct instructions for GPT: "List  $n$  descriptions with key properties to describe the [CLASS] in terms of appearance, color, shape, size, or material, etc. These descriptions will help visually distinguish the [CLASS] from other classes in the dataset. Each description should follow the format: 'a clean origami [CLASS]. it + descriptive contexts.'" With this instruction, we ask GPT to generate  $n$  detailed descriptions for each class, which are subsequently encoded into a dataset-wide knowledge base with CLIP’s text encoder. The knowledge base is denoted as  $\mathcal{T} = \{\Phi(e_i)\}_{i=1}^{n \times C}$ .  $e_i$  is the description from GPT,  $\Phi(\cdot)$  is CLIP’s text encoder and  $n \times C$  is the number of all descriptions. This knowledge base gathers descriptive properties for the whole dataset, building a strong foundation for the textual category representation.

**Implicit Attribute Hunting.** Instead of explicitly merging class-related knowledge into a single text embedding, we cluster this knowledge into generalized attributes and treat text prompting as an implicit attribute-hunting process. This has two main benefits: (1)  $n$  explicit descriptions may still be limited in covering all characteristics of the class. The clustered attributes efficiently capture shared contextual knowledge from other categories, supplementing missing information for target class recognition. (2) The generated descriptions inevitably contain redundant or noisy content. The use of attributes makes the knowledge more compact and representative, leading to precise text prompting.

To this end, we leverage a clustering algorithm to generate multiple centroids based on the knowledge base. Each cluster centroid is viewed as the implicit attribute that represents a group of descriptions sharing similar properties:

$$A = \text{Kmeans}(\mathcal{T}, B) = \{a_i\}_{i=1}^B, \quad (2)$$

where  $B$  is the number of centroids and kmeans algorithm [21] is used for clustering for simplicity.  $a_i \in \mathbb{R}^{D \times 1}$  represents the cluster centroid, i.e., the implicit attribute.

With the attribute feature space  $A$ , we first send the global template  $E_c$  into the text encoder of CLIP to generate global text embedding  $t_c \in \mathbb{R}^{D \times 1}$ .  $D$  is the channel dimension. Then  $t_c$  is leveraged to search for its most relevant attributes in the implicit attribute space. To exclude irrelevant attributes, we further propose to select TOPK attribute neighbors based on the similarity scores with  $t_c$ :

$$A_c = \{a_j : j \in \text{argmax}_{\text{TOPK}} \{t_c^T a_j\}_{j=1}^B\}. \quad (3)$$

Finally, we gently aggregate the implicit attribute neighbors according to the corresponding similarity weights to

$t_c$  and take the aggregated features as the complementary knowledge for textual semantic enrichment. The final text representation  $T_c \in \mathbb{R}^{D \times 1}$  is denoted as:

$$T_c = t_c + \lambda \sum_{j=1}^K \text{softmax}(t_c^T A_c) a_j, \quad (4)$$

where  $\lambda$  is the factor to balance the attribute information.

### 3.3. Visual Calibrations

**Static Visual Calibration.** Due to the image-text pairing nature of CLIP, the visual features lack fine-grained information, leading to unreasonable localization maps via patch-text alignment. To delve into this, let us review the self-attention mechanism of the original CLIP first. As shown in Fig. 2 (b), given the input image  $X \in \mathbb{R}^{3 \times \mathcal{H} \times \mathcal{W}}$ , we send it to the image encoder of CLIP, which includes 12 Attention layers in this work.  $\mathcal{H} \times \mathcal{W}$  is the image size. For the feature  $F_l \in \mathbb{R}^{D_s \times hw}$  from  $l$ -th layer of CLIP, it is first projected into three different spaces  $\{q, k, v\}$ , named query, key, and value, respectively.  $q, k$  and  $v$  have the same shape of  $D_s \times hw$ , where  $D_s$  and  $hw$  represents the channel dimension and sequence length. Then the attention map between  $q$  and  $k$  is calculated by measuring the similarity:

$$\text{SA}(q, k) = \text{softmax}\left(\frac{q^T k}{\sqrt{D_s}}\right), \quad (5)$$

where  $\text{SA}(\cdot)$  is the calculation of attention. Then the output features  $F_{l+1}$  are generated by aggregating the tokens of  $v$  according to similarity weights in the attention map.

However, due to the inherent image-text alignment of CLIP, the original q-k attention produces overly uniform attention maps, homogenizing diverse tokens from  $v$  to capture broad semantics for global image representation (see discussions in Sec. 4.4). It leads to inaccurate object recognition. MaskCLIP [47] holds a similar observation, supporting this claim by removing the final q-k attention layer and using  $v$  from the last layer as the visual output to preserve diversity. In our work, we choose to replace the suboptimal q-k attention with a straightforward Intra-correlation operation and focus on extracting fine-grained details from intermediate layers. This non-parametric approach effectively mines spatial semantics in intermediate  $\{q, k, v\}$  and avoids the smoothing effect of q-k attention, resulting in more consistent attention maps and improved object localization.

Specifically, instead of generating q-k correlation, Intra-correlation calculates the attention within each space of  $\{q, k, v\}$  across intermediate layers. The attention map  $S_{\text{attn}}^l \in \mathbb{R}^{hw \times hw}$  from  $l$ -th SVC layer is generated by:

$$S_{\text{attn}}^l = \sum w_i \text{SA}(O_i^l, O_i^l), O_i^l \in \{q^l, k^l, v^l\}, \quad (6)$$

where  $w_i$  is the contribution weight for different correlation maps.  $l \in \{12 - N, \dots, 12\}$  and  $N$  is the number of intermediate layers for this operation. Then  $S_{\text{attn}}^l$  and  $v^l$  are used to

generate the output features. Finally, the calibrated features  $P_s \in \mathbb{R}^{D \times h \times w}$  from the last layer is used to generate static CAM  $CAM_s$  with text embedding  $T_c$  via Eq. (1).

**Learnable Visual Calibration.** Although ExCEL generates comparable CAMs without training, its performance is still limited by the fixed features in CLIP. To further unleash the dense potential of CLIP, we design a lightweight adapter to dynamically calibrate the visual features with diverse details. This adapter only incorporates a distribution shift to calibrate the fixed features without changing CLIP’s pre-trained weights, thereby retaining CLIP’s transferability and enhancing its dense performance for WSSS.

Specifically, as shown in Fig. 2 (c), frozen features  $F_l$  from 1-12th layer of CLIP are extracted to learn a dynamic feature  $F_d$  via the adapter. The process is expressed as:

$$F_d = \text{Conv}(\text{Concate}[\delta_l(F_l)]_{l=1}^{12}), \quad (7)$$

where  $F_d \in \mathbb{R}^{D_d \times h_w}$ ,  $D_d$  is the channel dimension.  $\text{Conv}(\cdot)$  is the convolution layer,  $\text{Concate}[\cdot]$  is the concatenate operation that connects all features along channel dimension, and  $\delta_l(\cdot)$  is the individual MLP layer for each  $F_l$ . Then  $F_d$  is used to generate dynamic token relations by:

$$r = \alpha(\cos(F_d, F_d) - \beta \overline{\cos(F_d, F_d)}), \quad (8)$$

where  $r \in \mathbb{R}^{h_w \times h_w}$ ,  $\alpha$  and  $\beta$  are the scaling and shifting factors to adjust the relations, respectively.  $\overline{\cos(F_d, F_d)}$  means the mean value of similarity scores of  $F_d$ . It is designed to remove the irrelevant relations in low values by:

$$R_{ij} = \begin{cases} r_{ij}, & \text{if } r_{ij} \geq 0 \\ -inf, & \text{else} \end{cases}. \quad (9)$$

With the dynamic relation  $R \in \mathbb{R}^{h_w \times h_w}$ , we add it as a distribution bias to the static attention map  $S_{attn}^l$ , dynamically grouping the frozen tokens within related semantics and shifting the features towards denser distribution. The optimized attention map  $L_{attn}^l \in \mathbb{R}^{h_w \times h_w}$  is denoted as:

$$L_{attn}^l = S_{attn}^l + \text{softmax}(R). \quad (10)$$

Subsequently, we extract the dynamically calibrated features  $P_d \in \mathbb{R}^{D \times h \times w}$  from the last layer of LVC and generate dynamic CAMs with Eq. (1), which are then refined to final pseudo labels  $M_d$  for the segmentation.

### 3.4. Training Objectives

We formulate a diversity loss to supervise the learning of  $F_d$  in our LVC module. We first measure token correlations of  $F_d$  by calculating the self similarity:  $\hat{\mathcal{R}} = \text{sigmoid}(\cos(F_d, F_d))$ , where  $\text{sigmoid}(\cdot)$  is the activation function and  $\hat{\mathcal{R}} \in \mathbb{R}^{h_w \times h_w}$ . Then we refine  $CAM_s$  from SVC into static pseudo labels  $M_s$  and leverage its pixel-wise affinity to guide the diversifying of  $\hat{\mathcal{R}}$ . Specifically, if

the pixel with coordinate  $(i, j)$  shows the same pixel value as the pixel in  $(\varepsilon, \eta)$ , the token pair with the same coordinates on  $F_d$  is semantically related and its corresponding correlation logit on  $\hat{\mathcal{R}}$  should be maximized, and vice versa. The diversity loss can be formulated as:

$$\mathcal{L}_{\text{div}} = \frac{1}{N^+} \sum_{u^+ \in \hat{\mathcal{R}}^+} (1 - u^+) + \frac{1}{N^-} \sum_{u^- \in \hat{\mathcal{R}}^-} u^-, \quad (11)$$

where  $N^+/N^-$  are the number of positive and negative pairs,  $u^+/u^-$  are the positive and negative relation logits, and  $\hat{\mathcal{R}}^+/\hat{\mathcal{R}}^-$  are the positive and negative sets of logit on  $\hat{\mathcal{R}}$ , respectively. The diversity loss groups tokens with similar semantics and suppresses irrelevant ones, enhancing fine-grained details of visual features for precise text response.

In addition, ExCEL is streamlined as a single-stage method. We adopt a lightweight Transformer-based segmentation head [43] and directly take the frozen visual encoder of CLIP for segmentation. The dynamic pseudo labels are used as supervision with a cross-entropy loss  $\mathcal{L}_{\text{seg}}$ . The loss objectives of our ExCEL are formulated as:

$$\mathcal{L}_{\text{ExCEL}} = \mathcal{L}_{\text{seg}} + \gamma \mathcal{L}_{\text{div}}, \quad (12)$$

where  $\gamma$  is the weight factor. By efficiently training the adapter and a segmentation head, ExCEL achieves strong WSSS performance and significantly reduces training cost.

## 4. Experiments and Results

### 4.1. Experimental Settings

**Datasets and Metrics.** The proposed ExCEL is evaluated on PASCAL VOC 2012 [11] and MS COCO 2014 [19]. VOC contains 21 categories (1 for background). Following prior methods [10, 17, 39], the augmented dataset with 10,582, 1,449, and 1,456 images are used for training, validating, and testing, respectively. COCO includes 81 classes, in which 82,081 images are used for training and 40,137 images are for validating. Mean Intersection-Over-Union (mIoU) is used as the main evaluation metric.

**Implementation Details.** CLIP model with ViT-B [9] is used as ExCEL’s encoder, which is frozen during the training. For TSE module, we generate  $n = 20$  descriptions from GPT-4 for each category. The number of attribute embeddings  $B$  is set to 112 and 224 for PASCAL VOC and MS COCO, respectively. The SVC module is conducted in the last  $N = 5$  Transformer layers. Our decoder adopts a simple Transformer-based head [43]. Features  $F_l$  from each layer of CLIP are sent to it for the segmentation predictions. The scaling and shifting factors in Eq. (8) are set as 3.0 and 1.0, respectively. The loss weight  $\gamma$  is set as 0.1. Following [29, 35, 39], the AdamW optimizer is used for training the adapter and decoder. The learning rate is 1e-4 with a weight decay of 1e-2. The training iteration is set

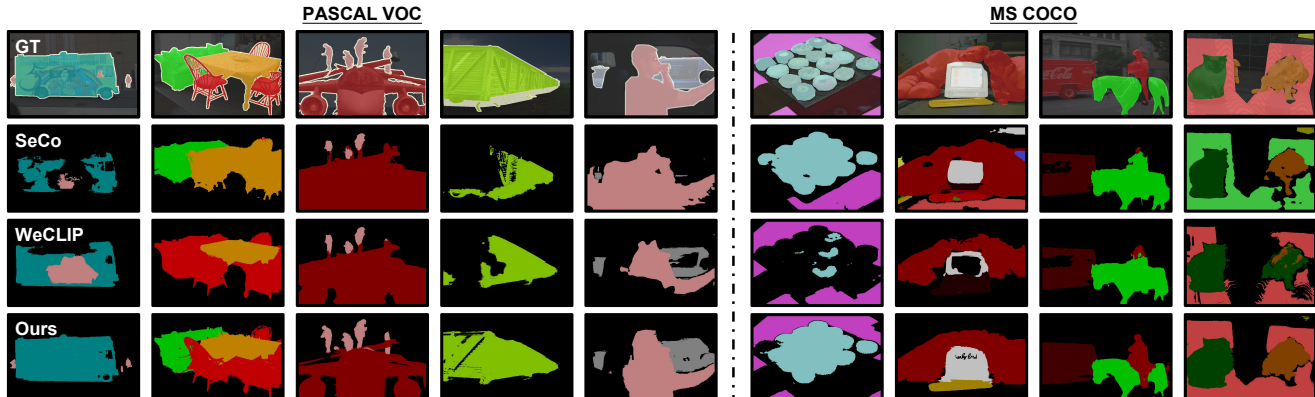


Figure 3. Segmentation visualizations of SeCo [39], WeCLIP [43] and ours on VOC and COCO. ExCEL segments objects more precisely.

Table 1. Segmentation comparisons on VOC and COCO. Net. is the backbone for segmentation. Sup. is the supervision type.  $\mathcal{I}$ : image-level labels.  $\mathcal{SA}$ : saliency maps.  $\mathcal{L}$ : language.

Method	Sup.	Net.	VOC		COCO
			Val	Test	Val
<i>Multi-stage WSSS methods.</i>					
L2G [14] CVPR'2022	$\mathcal{I} + \mathcal{SA}$	RN101	72.1	71.7	44.2
RCA [49] CVPR'2023	$\mathcal{I} + \mathcal{SA}$	RN38	72.2	72.8	36.8
OCR [7] CVPR'2023	$\mathcal{I}$	RN38	72.7	72.0	42.5
BECO [26] CVPR'2023	$\mathcal{I}$	RN101	73.7	73.5	45.1
MCTformer+ [38] TPAMI'2024	$\mathcal{I}$	RN38	74.0	73.6	45.2
CTI [41] CVPR'2024	$\mathcal{I}$	RN101	74.1	73.2	45.4
CLIMS [36] CVPR'2022	$\mathcal{I} + \mathcal{L}$	RN101	70.4	70.0	-
CLIP-ES [20] CVPR'2023	$\mathcal{I} + \mathcal{L}$	RN101	72.2	72.8	45.4
PSDPM [45] CVPR'2024	$\mathcal{I} + \mathcal{L}$	RN101	74.1	74.9	47.2
CPAL [31] CVPR'2024	$\mathcal{I} + \mathcal{L}$	RN101	74.5	74.7	46.8
<i>Single-stage WSSS methods.</i>					
AFA [28] CVPR'2022	$\mathcal{I}$	MiT-B1	66.0	66.3	38.9
ViT-PCM [27] ECCV'2022	$\mathcal{I}$	ViT-B	70.3	70.9	-
ToCo [29] CVPR'2023	$\mathcal{I}$	ViT-B	71.1	72.2	42.3
DuPL [35] CVPR'2024	$\mathcal{I}$	ViT-B	73.3	72.8	44.6
SeCo [39] CVPR'2024	$\mathcal{I}$	ViT-B	74.0	73.8	46.7
DIAL [13] ECCV'2024	$\mathcal{I} + \mathcal{L}$	ViT-B	74.5	74.9	44.4
WeCLIP [43] CVPR'2024	$\mathcal{I} + \mathcal{L}$	ViT-B	76.4	77.2	47.1
ExCEL(w/o CRF)	$\mathcal{I} + \mathcal{L}$	ViT-B	77.2	77.3	49.3
ExCEL (Ours)	$\mathcal{I} + \mathcal{L}$	ViT-B	78.4	78.5	50.3

as 30,000 for VOC and 100,000 for COCO. Please refer to Supplementary Materials for more details.

## 4.2. Comparisons with State-of-the-art Methods

**Performance of Semantic Segmentation.** Tab. 1 shows segmentation comparisons between our ExCEL and recent methods on VOC and COCO. The single-stage ExCEL achieves 78.4% and 78.5% mIoU on VOC val set and test set, which even significantly outperforms the sophisticated multi-stage methods by at least 3.9% and 3.6% mIoU, respectively. For more complicated benchmark COCO, ExCEL achieves 50.3% mIoU on val set, which brings a noticeable 3.2% increase over the CLIP-based state-of-the-art (SOTA) WeCLIP. In addition, without time-consuming post-processing techniques, such as CRF [15], ExCEL still

Table 2. CAM seed comparisons on VOC train set.  $\mathcal{M}$ : multi-stage methods.  $\mathcal{S}$ : single-stage methods. †: our reproduction following official codes. ExCEL\*: ExCEL in a training-free manner.

Method	Type	Sup.	Net.	VOC
				Train
<i>Training-free WSSS methods.</i>				
CLIP-ES [20] CVPR'2023	$\mathcal{M}$	$\mathcal{I} + \mathcal{L}$	ViT-B	70.8
ExCEL* (Ours)	$\mathcal{S}$	$\mathcal{I} + \mathcal{L}$	ViT-B	74.6
<i>Training-required WSSS methods.</i>				
ReCAM [6] CVPR'2022	$\mathcal{M}$	$\mathcal{I}$	RN101	54.8
FPR [3] CVPR'2023	$\mathcal{M}$	$\mathcal{I}$	RN101	63.8
LPCAM [5] CVPR'2023	$\mathcal{M}$	$\mathcal{I}$	RN50	65.3
MCTformer+ [38] TPAMI'2024	$\mathcal{M}$	$\mathcal{I}$	RN38	68.8
SFC [44] AAAI'2024	$\mathcal{M}$	$\mathcal{I}$	RN101	64.7
CTI [41] CVPR'2024	$\mathcal{M}$	$\mathcal{I}$	RN101	69.5
AFA [28] CVPR'2022	$\mathcal{S}$	$\mathcal{I}$	MiT-B1	65.0
ViT-PCM [27] ECCV'2022	$\mathcal{S}$	$\mathcal{I}$	ViT-B	67.7
†ToCo [29] CVPR'2023	$\mathcal{S}$	$\mathcal{I}$	ViT-B	71.6
†DuPL [35] CVPR'2024	$\mathcal{S}$	$\mathcal{I}$	ViT-B	75.0
SeCo [39] CVPR'2024	$\mathcal{S}$	$\mathcal{I}$	ViT-B	74.8
CLIMS [36] CVPR'2022	$\mathcal{M}$	$\mathcal{I} + \mathcal{L}$	RN101	56.6
POLE [22] WACV'2023	$\mathcal{M}$	$\mathcal{I} + \mathcal{L}$	RN50	59.0
CPAL [31] CVPR'2024	$\mathcal{M}$	$\mathcal{I} + \mathcal{L}$	RN101	71.9
DIAL [13] ECCV'2024	$\mathcal{S}$	$\mathcal{I} + \mathcal{L}$	ViT-B	75.2
†WeCLIP [43] CVPR'2024	$\mathcal{S}$	$\mathcal{I} + \mathcal{L}$	ViT-B	75.4
ExCEL (Ours)	$\mathcal{S}$	$\mathcal{I} + \mathcal{L}$	ViT-B	78.0

maintains consistent superiority over SOTAs with CRF.

The qualitative comparisons on VOC and COCO are shown in Fig. 3. By densely matching the patches and texts, ExCEL consistently demonstrates more precise object segmentation than recent methods in an image-text paradigm.

**Evaluation of CAM Seeds.** Tab. 2 reports the quality of raw CAM seeds on VOC train set. Compared with recent methods, ExCEL achieves 74.6% mIoU in a training-free setup, outperforming CLIP-ES by 3.8% and performing comparably to most training-required methods. With the optimized LVC module, ExCEL further boosts CAM quality to 78.0%, surpassing SOTAs in the image-text paradigm by at least 2.6%. In addition, visual comparisons in Fig. 4 (e-h) also plainly illustrates that ExCEL generates better CAMs with the designed patch-text alignment paradigm.

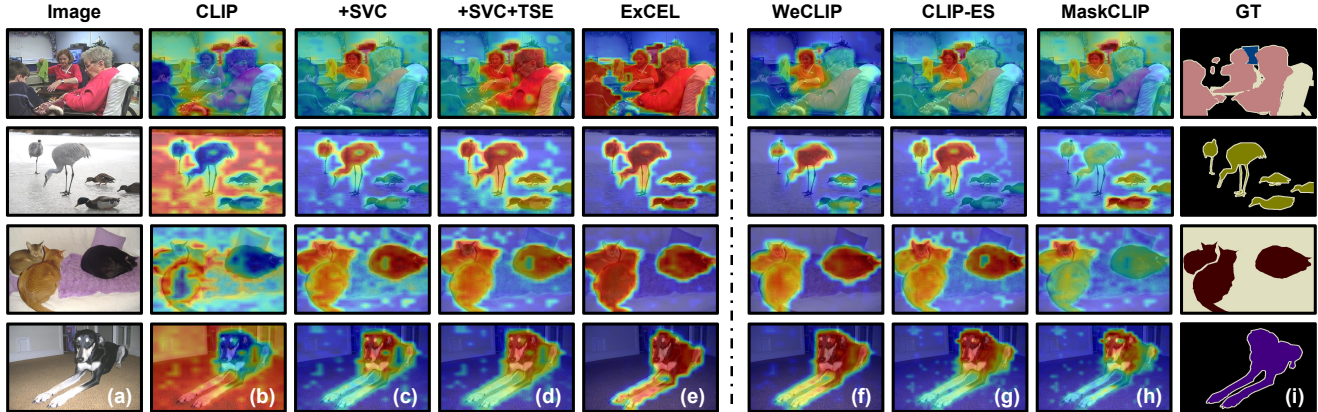


Figure 4. CAM visualizations on VOC train set. (a) Image. (b-e) Ablative visualizations of proposed modules. (e-h) Qualitative comparisons of (e) ExCEL and recent CLIP-based methods, i.e., (f) WeCLIP [43], (g) CLIP-ES [20] and (h) MaskCLIP [47]. (i) Ground truth.

Table 3. Ablation study of ExCEL on VOC val set.

Conditions	SVC	TSE	LVC	Precision	Recall	mIoU
Baseline (CLIP)				18.8	21.3	12.1
w/ SVC	✓			81.2	86.2	72.5
w/o LVC	✓	✓		80.7	89.8	74.7
w/o TSE	✓		✓	83.7	86.3	75.1
<b>ExCEL</b>	✓	✓	✓	<b>85.0</b>	<b>88.4</b>	<b>77.2</b>

Table 4. Ablation study of attribute number  $B$  on VOC val set.

Number of Attr	None	32	64	<b>112</b>	144	196
mIoU	75.1	75.8	76.2	<b>77.2</b>	77.0	76.5

Table 5. Ablation study of VC module on VOC train set.

Conditions	q-k	v	I.C.	M.C.	LVC	Precision	Recall	mIoU
Baseline (CLIP)	✓					18.0	21.8	11.2
MaskCLIP		✓				77.1	80.9	65.8
w/ I.C.			✓			79.1	84.7	69.7
SVC			✓	✓		82.2	88.2	74.6
<b>ExCEL</b>			✓	✓	✓	<b>86.6</b>	<b>87.9</b>	<b>78.0</b>

### 4.3. Ablation Studies

**Efficacy of Key Components.** Quantitative ablative experiments of ExCEL are reported in Tab. 3. The baseline is the vanilla CLIP using our training settings, which only achieves 12.1% mIoU for segmentation. Our SVC module replaces the q-k attention with Intra-correlation from the intermediate layers. The performance increases to 72.5%. TSE module enriches the semantics of text representation for robust visual recognition. Introducing TSE brings a 3.6% recall increase compared to the original text templates. LVC module provides a dynamic shift to diversify the features. It further benefits SVC’s segmentation performance to 75.1% mIoU. With all these enhancements, ExCEL generates 77.2% mIoU for segmentation.

Qualitative ablation results are further illustrated in Fig. 4 (b-e) to evaluate the efficacy of our modules. In Fig. 4 (b), the CLIP baseline produces inaccurate CAMs with mis-

localized activation. SVC corrects token relations and preserves fine-grained details, effectively suppressing false activations, as seen in Fig. 4 (c). TSE incorporates comprehensive textual attributes into the text representation, enhancing patch-text matching and producing more complete CAMs, shown in Fig. 4 (d). LVC dynamically optimizes attention maps, further improving CAM accuracy and completeness, as illustrated in Fig. 4 (e). Both quantitative and qualitative results confirm the effectiveness of our modules.

**Effectiveness of Implicit Attributes.** Tab. 4 analyzes the effect of varying the number of clustering attributes. ‘None’ means no clustering and we explicitly fuse the  $n$  description embeddings for each class. It shows that the performance drops from 77.2% to 75.1%, which validates the efficacy of implicit attributes and its superiority over explicit descriptions. With this operation, we can expand the representation of 20 classes up to 196 attributes or more, greatly enhancing text semantics. It reports that ExCEL achieves more favorable performance when  $B$  is set to 112.

**Effectiveness of Visual Calibrations.** Tab. 5 compares different strategies in VC module for CAM generation. I.C. refers to Intra-correlation in the last layer, and M.C. (Intermediate Calibration) applies I.C. across intermediate layers. Vanilla q-k attention in CLIP loses diversity and cannot generate reasonable CAMs.  $v$  contains fine-grained knowledge and MaskCLIP improves CAMs to 65.8% by using  $v$  from the last layer. In contrast, our I.C. and M.C. focus on mining diverse knowledge from intermediate layers and boost the performance to 69.7% and 74.6%. In addition, introducing LVC module raises the final performance to 78.0%. Results in Tab. 5 and corresponding visualizations in Fig. 4 clearly highlight the efficacy of our components.

### 4.4. Further Analysis

**Hyper-parameter Analysis.** Hyper-parameters, such as  $TOP-K$ , scaling factors  $\alpha$  and  $\beta$ , and the number of SVC layers  $N$ , etc., are discussed in **Supplementary Materials**.

Table 6. Comparisons with the fully-supervised counterparts on VOC val set.  $\mathcal{F}$ :fully-supervised. ViT-B\*: pretrained from CLIP.

Methods	Type	Sup.	Net.	Val	Ratio
DeepLabV2 [4] TPAMI'2017	-	$\mathcal{F}$	RN101	77.7	-
DeepLabV2 [4] TPAMI'2017	-	$\mathcal{F}$	ViT-B	82.3	-
WeCLIP-Full [43] CVPR'2024	-	$\mathcal{F}$	ViT-B*	81.6	-
CLIMS [36] CVPR'2022	$\mathcal{M}$	$\mathcal{I} + \mathcal{L}$	RN101	70.4	90.6%
CLIP-ES [20] CVPR'2023	$\mathcal{M}$	$\mathcal{I} + \mathcal{L}$	RN101	72.2	92.9%
CPAL [31] CVPR'2024	$\mathcal{M}$	$\mathcal{I} + \mathcal{L}$	RN101	74.5	95.9%
ToCo [29] CVPR'2024	$\mathcal{S}$	$\mathcal{I}$	ViT-B	71.1	86.4%
DuPL [35] CVPR'2024	$\mathcal{S}$	$\mathcal{I}$	ViT-B	73.3	89.1%
SeCo [43] CVPR'2024	$\mathcal{S}$	$\mathcal{I}$	ViT-B	74.0	89.9%
DIAL [13] ECCV'2024	$\mathcal{S}$	$\mathcal{I} + \mathcal{L}$	ViT-B	74.5	90.5%
WeCLIP [43] CVPR'2024	$\mathcal{S}$	$\mathcal{I} + \mathcal{L}$	ViT-B*	76.4	93.6%
<b>ExCEL (Ours)</b>	$\mathcal{S}$	$\mathcal{I} + \mathcal{L}$	<b>ViT-B*</b>	<b>78.4</b>	<b>96.1%</b>

Table 7. Training efficiency comparisons on VOC train (CAM) and val set (Seg). All experiments are conducted on RTX 3090.

Method	Type	Training Time	GPU	CAM	Seg
CLIMS [36] CVPR'2022	$\mathcal{M}$	1068 mins	18.0 G	56.6	70.4
CLIP-ES [20] CVPR'2023	$\mathcal{M}$	420 mins	12.0 G	70.8	72.2
MCTformer+ [38] TPAMI'2024	$\mathcal{M}$	1496 mins	18.0 G	68.8	74.0
ToCo [29] CVPR'2023	$\mathcal{S}$	506 mins	17.9 G	71.6	71.1
DuPL [35] CVPR'2024	$\mathcal{S}$	508 mins	14.9 G	75.0	73.3
SeCo [39] CVPR'2024	$\mathcal{S}$	407 mins	17.6 G	74.8	74.0
WeCLIP [43] CVPR'2024	$\mathcal{S}$	270 mins	6.2 G	75.4	76.4
<b>ExCEL* (Training-free)</b>	$\mathcal{S}$	-	<b>2.9 G</b>	<b>74.6</b>	-
<b>ExCEL (Ours)</b>	$\mathcal{S}$	<b>90 mins</b>	<b>3.2 G</b>	<b>78.0</b>	<b>78.4</b>

**Fully-supervised Counterparts.** Tab. 6 presents a fairness comparison between WSSS methods and their fully-supervised counterparts using the same segmentation backbone. With CLIP’s visual encoder as the backbone, ExCEL achieves 78.4% mIoU, reaching 96.1% of the fully-supervised performance. It significantly outperforms CLIP-based WeCLIP by 2.5% and demonstrates ExCEL’s advantage over other multi-stage CLIP-based methods as well.

**Training Efficiency Analysis.** Our method only trains the adapter and decoder in a single-stage paradigm. Tab. 7 compares the training efficiency between ExCEL and recent methods. Without training, ExCEL requires just 2.9 GB of GPU memory and generates comparable CAMs to recent SOTAs. When training is included, the entire pipeline only takes 90 minutes and 3.2 GB of memory for SOTA performance. ExCEL just requires 6.0% training time of multi-stage MCTformer+ and 33.3% of single-stage WeCLIP, highlighting ExCEL’s remarkable training efficiency.

**Attribute Response Analysis.** We treat text prompting as an implicit attribute-hunting process to comprehensively enrich text representation semantics. To evaluate if the clustered attributes capture distinct object characteristics, we visualize 5 implicit attributes based on similarity scores. As shown in Fig. 5, given instances of  $\{aeroplane\}$  and  $\{train\}$ , our attributes highlight different object parts, which clearly validates that our TSE module enhances inte-

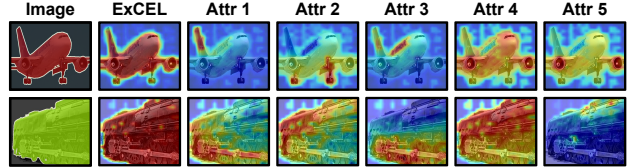


Figure 5. Implicit attribute responses. Based on the TOPK similarity scores, 5 attributes are sampled for visualizations.

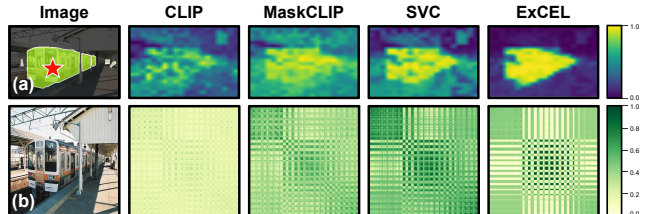


Figure 6. Comparisons of attention maps from the last visual encoder layer. (a) Attention features from the query patches (marked by red stars). (b) Token relations measured by cosine similarity.

gral visual responses by gathering relevant semantics.

**Feature Representation Analysis.** CLIP lacks fine-grained details, leading to inaccurate patch-text responses. To explore further, we visualize the self-attention features in Fig. 6 (a). Given the query patch (red star), CLIP’s q-k attention falls short in generating diverse features, supporting our claim in Sec. 3.3. MaskCLIP observes that  $v$  keeps diversity and takes it from the last layer for visual response. We visualize it by calculating v-v attention. Although effective, MaskCLIP still misses fine granularity. Instead, SVC calculates attention within each space and implements it from intermediate layers. LVC further diversifies the features with a dynamic adapter, both of which effectively generate features with clear boundaries and spatial details.

Additionally, we explore the pairwise token relations in Fig. 6 (b). Unlike the smoother attention maps of CLIP or MaskCLIP, our approach distinctly groups tokens with similar semantics, aligning pairwise similarities with corresponding semantics. This validates that ExCEL successfully enhances the frozen features of CLIP by calibrating it towards distributions with more diverse spatial information.

## 5. Conclusion

In this paper, we propose ExCEL, a novel patch-text alignment method to explore CLIP’s dense knowledge for WSSS, which provides a different insight to generate better pseudo labels based on CLIP. To this end, Text Semantic Enrichment (TSE) and Visual Calibration (VC) modules are designed to improve the dense alignment across text and vision modalities. In addition, ExCEL generates CAMs in both training-free and efficient training modes, calibrating CLIP without altering its pre-trained weights. It retains CLIP’s transferability while significantly reducing training cost. We believe ExCEL can inspire more future research to unlock CLIP’s dense capabilities in the WSSS field.



## 6. Acknowledgments

This work was supported by the National Natural Science Foundation of China under Grant No.82372097, Shanghai Sailing Program under Grant 22YF1409300, International Science and Technology Cooperation Program under the 2023 Shanghai Action Plan for Science under Grant 23410710400, Taishan Scholars Program under Grant NO.tsqn202408245.

## References

- [1] Jiwoon Ahn and Suha Kwak. Learning pixel-level semantic affinity with image-level supervision for weakly supervised semantic segmentation. In *CVPR*, pages 4981–4990, 2018. 1
- [2] Amy Bearman, Olga Russakovsky, Vittorio Ferrari, and Li Fei-Fei. What’s the point: Semantic segmentation with point supervision. In *Computer Vision–ECCV 2016: 14th European Conference, Amsterdam, The Netherlands, October 11–14, 2016, Proceedings, Part VII 14*, pages 549–565. Springer, 2016. 1
- [3] Liyi Chen, Chenyang Lei, Ruihuang Li, Shuai Li, Zhaoxiang Zhang, and Lei Zhang. Fpr: False positive rectification for weakly supervised semantic segmentation. In *ICCV*, pages 1108–1118, 2023. 6
- [4] Liang-Chieh Chen, George Papandreou, Iasonas Kokkinos, Kevin Murphy, and Alan L Yuille. Deeplab: Semantic image segmentation with deep convolutional nets, atrous convolution, and fully connected crfs. *IEEE transactions on pattern analysis and machine intelligence*, 40(4):834–848, 2017. 8
- [5] Zhaozheng Chen and Qianru Sun. Extracting class activation maps from non-discriminative features as well. In *CVPR*, pages 3135–3144, 2023. 1, 6
- [6] Zhaozheng Chen, Tan Wang, Xiongwei Wu, Xian-Sheng Hua, Hanwang Zhang, and Qianru Sun. Class re-activation maps for weakly-supervised semantic segmentation. In *CVPR*, pages 969–978, 2022. 6
- [7] Zesen Cheng, Pengchong Qiao, Kehan Li, Siheng Li, Pengxu Wei, Xiangyang Ji, Li Yuan, Chang Liu, and Jie Chen. Out-of-candidate rectification for weakly supervised semantic segmentation. In *Proceedings of the IEEE/CVF Conference on Computer Vision and Pattern Recognition*, pages 23673–23684, 2023. 1, 6
- [8] Jifeng Dai, Kaiming He, and Jian Sun. Boxesup: Exploiting bounding boxes to supervise convolutional networks for semantic segmentation. In *ICCV*, pages 1635–1643, 2015. 1
- [9] Alexey Dosovitskiy, Lucas Beyer, Alexander Kolesnikov, Dirk Weissenborn, Xiaohua Zhai, Thomas Unterthiner, Mostafa Dehghani, Matthias Minderer, Georg Heigold, Sylvain Gelly, et al. An image is worth 16x16 words: Transformers for image recognition at scale. *arXiv preprint arXiv:2010.11929*, 2020. 5
- [10] Ye Du, Zehua Fu, Qingjie Liu, and Yunhong Wang. Weakly supervised semantic segmentation by pixel-to-prototype contrast. In *CVPR*, pages 4320–4329, 2022. 5
- [11] Mark Everingham, SM Ali Eslami, Luc Van Gool, Christopher KI Williams, John Winn, and Andrew Zisserman. The pascal visual object classes challenge: A retrospective. *IJCV*, 111:98–136, 2015. 5
- [12] Peng Gao, Shijie Geng, Renrui Zhang, Teli Ma, Rongyao Fang, Yongfeng Zhang, Hongsheng Li, and Yu Qiao. Clip-adapter: Better vision-language models with feature adapters. *International Journal of Computer Vision*, 132(2): 581–595, 2024. 2
- [13] Soojin Jang, Jungmin Yun, Junehyoung Kwon, Eunju Lee, and Youngbin Kim. Dial: Dense image-text alignment for weakly supervised semantic segmentation. *arXiv preprint arXiv:2409.15801*, 2024. 6, 8
- [14] Peng-Tao Jiang, Yuqi Yang, Qibin Hou, and Yunchao Wei. L2g: A simple local-to-global knowledge transfer framework for weakly supervised semantic segmentation. In *Proceedings of the IEEE/CVF conference on computer vision and pattern recognition*, pages 16886–16896, 2022. 6
- [15] Philipp Krähenbühl and Vladlen Koltun. Efficient inference in fully connected crfs with gaussian edge potentials. *NeurIPS*, 24, 2011. 6
- [16] Jungbeom Lee, Jihun Yi, Chaehun Shin, and Sungroh Yoon. Bbam: Bounding box attribution map for weakly supervised semantic and instance segmentation. In *Proceedings of the IEEE/CVF conference on computer vision and pattern recognition*, pages 2643–2652, 2021. 1
- [17] Xueyi Li, Tianfei Zhou, Jianwu Li, Yi Zhou, and Zhaoxiang Zhang. Group-wise semantic mining for weakly supervised semantic segmentation. In *AAAI*, pages 1984–1992, 2021. 5
- [18] Di Lin, Jifeng Dai, Jiaya Jia, Kaiming He, and Jian Sun. Scribblesup: Scribble-supervised convolutional networks for semantic segmentation. In *CVPR*, pages 3159–3167, 2016. 1
- [19] Tsung-Yi Lin, Michael Maire, Serge Belongie, James Hays, Pietro Perona, Deva Ramanan, Piotr Dollár, and C Lawrence Zitnick. Microsoft coco: Common objects in context. In *Computer Vision–ECCV 2014: 13th European Conference, Zurich, Switzerland, September 6–12, 2014, Proceedings, Part V 13*, pages 740–755. Springer, 2014. 5
- [20] Yuqi Lin, Minghao Chen, Wenxiao Wang, Boxi Wu, Ke Li, Binbin Lin, Haifeng Liu, and Xiaofei He. Clip is also an efficient segmenter: A text-driven approach for weakly supervised semantic segmentation. *arXiv preprint arXiv:2212.09506*, 2022. 1, 3, 6, 7, 8
- [21] Stuart Lloyd. Least squares quantization in pcm. *IEEE transactions on information theory*, 28(2):129–137, 1982. 4
- [22] Balamurali Murugesan, Rukshanda Hussain, Rajarshi Bhattacharya, Ismail Ben Ayed, and Jose Dolz. Prompting classes: exploring the power of prompt class learning in weakly supervised semantic segmentation. In *Proceedings of the IEEE/CVF Winter Conference on Applications of Computer Vision*, pages 291–302, 2024. 6
- [23] Pedro O Pinheiro and Ronan Collobert. From image-level to pixel-level labeling with convolutional networks. In *CVPR*, pages 1713–1721, 2015. 1
- [24] Alec Radford, Jong Wook Kim, Chris Hallacy, Aditya Ramesh, Gabriel Goh, Sandhini Agarwal, Girish Sastry, Amanda Askell, Pamela Mishkin, Jack Clark, et al. Learning transferable visual models from natural language supervi-

- sion. In *International conference on machine learning*, pages 8748–8763. PMLR, 2021. 1, 2
- [25] Yongming Rao, Wenliang Zhao, Guangyi Chen, Yansong Tang, Zheng Zhu, Guan Huang, Jie Zhou, and Jiwen Lu. Denseclip: Language-guided dense prediction with context-aware prompting. In *Proceedings of the IEEE/CVF conference on computer vision and pattern recognition*, pages 18082–18091, 2022. 2
- [26] Shenghai Rong, Bohai Tu, Zilei Wang, and Junjie Li. Boundary-enhanced co-training for weakly supervised semantic segmentation. In *Proceedings of the IEEE/CVF Conference on Computer Vision and Pattern Recognition*, pages 19574–19584, 2023. 6
- [27] Simone Rossetti, Damiano Zappia, Marta Sanzari, Marco Schaerf, and Fiora Pirri. Max pooling with vision transformers reconciles class and shape in weakly supervised semantic segmentation. In *ECCV*, pages 446–463. Springer, 2022. 6
- [28] Lixiang Ru, Yibing Zhan, Baosheng Yu, and Bo Du. Learning affinity from attention: end-to-end weakly-supervised semantic segmentation with transformers. In *Proceedings of the IEEE/CVF Conference on Computer Vision and Pattern Recognition*, pages 16846–16855, 2022. 1, 6
- [29] Lixiang Ru, Heliang Zheng, Yibing Zhan, and Bo Du. Token contrast for weakly-supervised semantic segmentation. *arXiv preprint arXiv:2303.01267*, 2023. 2, 5, 6, 8
- [30] Ramprasaath R Selvaraju, Michael Cogswell, Abhishek Das, Ramakrishna Vedantam, Devi Parikh, and Dhruv Batra. Grad-cam: Visual explanations from deep networks via gradient-based localization. In *Proceedings of the IEEE international conference on computer vision*, pages 618–626, 2017. 2
- [31] Feilong Tang, Zhongxing Xu, Zhaojun Qu, Wei Feng, Xingjian Jiang, and Zongyuan Ge. Hunting attributes: Context prototype-aware learning for weakly supervised semantic segmentation. In *Proceedings of the IEEE/CVF Conference on Computer Vision and Pattern Recognition*, pages 3324–3334, 2024. 6, 8
- [32] Paul Vernaza and Manmohan Chandraker. Learning random-walk label propagation for weakly-supervised semantic segmentation. In *CVPR*, pages 7158–7166, 2017. 1
- [33] Xiang Wang, Shaodi You, Xi Li, and Huimin Ma. Weakly-supervised semantic segmentation by iteratively mining common object features. In *CVPR*, pages 1354–1362, 2018. 1
- [34] Yuanchen Wu, Xiaoqiang Li, Jide Li, Pinpin Zhu, Shaohua Zhang, et al. Dino is also a semantic guider: Exploiting class-aware affinity for weakly supervised semantic segmentation. In *ACM Multimedia 2024*. 2
- [35] Yuanchen Wu, Xichen Ye, Kequan Yang, Jide Li, and Xiaoqiang Li. Dupl: Dual student with trustworthy progressive learning for robust weakly supervised semantic segmentation. In *CVPR*, pages 3534–3543, 2024. 5, 6, 8
- [36] Jinheng Xie, Xianxu Hou, Kai Ye, and Linlin Shen. Clims: cross language image matching for weakly supervised semantic segmentation. In *Proceedings of the IEEE/CVF Conference on Computer Vision and Pattern Recognition*, pages 4483–4492, 2022. 1, 3, 6, 8
- [37] Lian Xu, Wanli Ouyang, Mohammed Bennamoun, Farid Boussaid, and Dan Xu. Multi-class token transformer for weakly supervised semantic segmentation. In *Proceedings of the IEEE/CVF Conference on Computer Vision and Pattern Recognition*, pages 4310–4319, 2022. 2
- [38] Lian Xu, Mohammed Bennamoun, Farid Boussaid, Hamid Laga, Wanli Ouyang, and Dan Xu. Mctformer+: Multi-class token transformer for weakly supervised semantic segmentation. *IEEE transactions on pattern analysis and machine intelligence*, 2024. 6, 8
- [39] Zhiwei Yang, Kexue Fu, Minghong Duan, Linhao Qu, Shuo Wang, and Zhijian Song. Separate and conquer: Decoupling co-occurrence via decomposition and representation for weakly supervised semantic segmentation. In *CVPR*, pages 3606–3615, 2024. 2, 5, 6, 8
- [40] Zhiwei Yang, Yucong Meng, Kexue Fu, Shuo Wang, and Zhijian Song. Tackling ambiguity from perspective of uncertainty inference and affinity diversification for weakly supervised semantic segmentation. *arXiv preprint arXiv:2404.08195*, 2024. 1
- [41] Sung-Hoon Yoon, Hoyong Kwon, Hyeonseong Kim, and Kuk-Jin Yoon. Class tokens infusion for weakly supervised semantic segmentation. In *Proceedings of the IEEE/CVF Conference on Computer Vision and Pattern Recognition*, pages 3595–3605, 2024. 6
- [42] Bingfeng Zhang, Xuru Gao, Siyue Yu, and Weifeng Liu. Enhanced online cam: Single-stage weakly supervised semantic segmentation via collaborative guidance. *Pattern Recognition*, 156:110787, 2024. 2
- [43] Bingfeng Zhang, Siyue Yu, Yunchao Wei, Yao Zhao, and Jimin Xiao. Frozen clip: A strong backbone for weakly supervised semantic segmentation. In *Proceedings of the IEEE/CVF Conference on Computer Vision and Pattern Recognition*, pages 3796–3806, 2024. 2, 3, 5, 6, 7, 8
- [44] Xinqiao Zhao, Feilong Tang, Xiaoyang Wang, and Jimin Xiao. Sfc: Shared feature calibration in weakly supervised semantic segmentation. In *Proceedings of the AAAI Conference on Artificial Intelligence*, pages 7525–7533, 2024. 2, 6
- [45] Xinqiao Zhao, Ziqian Yang, Tianhong Dai, Bingfeng Zhang, and Jimin Xiao. Psdpm: Prototype-based secondary discriminative pixels mining for weakly supervised semantic segmentation. In *CVPR*, pages 3437–3446, 2024. 6
- [46] Bolei Zhou, Aditya Khosla, Agata Lapedriza, Aude Oliva, and Antonio Torralba. Learning deep features for discriminative localization. In *CVPR*, pages 2921–2929, 2016. 1
- [47] Chong Zhou, Chen Change Loy, and Bo Dai. Extract free dense labels from clip. In *European Conference on Computer Vision*, pages 696–712. Springer, 2022. 3, 4, 7
- [48] Kaiyang Zhou, Jingkang Yang, Chen Change Loy, and Ziwei Liu. Learning to prompt for vision-language models. *International Journal of Computer Vision*, 130(9):2337–2348, 2022. 2
- [49] Tianfei Zhou, Meijie Zhang, Fang Zhao, and Jianwu Li. Regional semantic contrast and aggregation for weakly supervised semantic segmentation. In *CVPR*, pages 4299–4309, 2022. 6